2011년 8월

석사학위논문

Prediction of Axial DNBR Distribution in a Hot Nuclear Fuel Rod Using Support Vector Regression

조 선 대 학 교 대 학 원

원 자 력 공 학 과

김 동 수

Prediction of Axial DNBR Distribution in a Hot Nuclear Fuel Rod Using Support Vector Regression

- Support Vector Regression을 이용한 고온봉에서의 축방향 DNBR 분포 예측 -

2011년 8월 25일

조 선 대 학 교 대 학 원

원 자 력 공 학 과

김 동 수

Prediction of Axial DNBR Distribution in a Hot Nuclear Fuel Rod Using Support Vector Regression

지도교수 나 만 균

이 논문을 공학 석사학위신청 논문으로 제출함.

2011년 4월

조 선 대 학 교 대 학 원

원 자 력 공 학 과

김 동 수

김동수의 석사학위 논문을 인준함

위원장　조선대학교　교수　김 숭 평　(인)

위　원　조선대학교　부교수　김 진 원　(인)

위　원　조선대학교　교수　나 만 균　(인)

2011년　5월

조 선 대 학 교 대 학 원

CONTENTS

List of Tables

List of Figures

Abstract

Prediction of Axial DNBR Distribution in a Hot Nuclear Fuel Rod Using Support Vector Regression

김 동 수
지도 교수 : 나 만 균
조선대학교 일반대학원 원자력공학과

비등위기 및 핵연료 피복관 용융을 방지하기 위한 지표인자인 핵비등이탈율 계산은 안전성 측면에서 계속 모니터링 되어야 하는 매우 중요한 인자이다. 현재 원자력 발전소에 있는 대부분의 원자로 노심보호 시스템들은 핵비등이탈을 예방하기 위하여 고온봉의 허위 위치(pseudo position)에서의 최소 핵비등이탈률을 사용하는데 이것은 핵비등이탈을 예측하는데 보수적인 결과를 초래하여 원자력발전소의 운전여유도를 감소시킨다. 따라서, 본 논문에서는 데이터 기반 인공지능 방법 중 하나인 Support Vector Regression 방법을 이용하여 고온봉의 실제 위치(actual position)에서의 DNBR 분포를 예측하였다. 위의 SVR 모델은 학습데이터를 이용하여 개발되었으며, 학습데이터와 독립적인 시험데이터에 의해 성능이 증명되었다. 또한 더 많은 정보를 가지고 있는 학습데이터를 선정하기 위해 Subtractive Clustering 방법이 사용되었다. 제안된 DNB 예측 알고리즘은 영광 원자력발전소 3호기의 시뮬레이션으로부터 획득된 수많은 데이터를 사용하여 증명되었다. 개발된 모델의 적용 결과, 고온봉의 13개 축방향 위치에서 평균 RMS 오차는 0.87%였다. 이 결과는 개발된 모델이 DNBR을 정확히 예측한다는 것을 보여주며, 실제 발전소의 노심보호 및 감시계통에 적용가능성을 제공할 수 있을 것으로 기대된다.

Ⅰ. Introduction

The pressurized water reactors (PWRs) generally operate in the nucleate boiling regime. However, if the fuel rod is operating at high power density, the nucleate boiling may eventually reach the film boiling accompanied by severe reduction of heat transfer capability. The conversion of the nucleate boiling into the film boiling induces the boiling crisis that in the long run may cause fuel clad melting. This type of boiling crisis is a phenomenon called Departure from Nucleate Boiling (DNB). The DNB phenomena overheat the cladding and fuel pellet if the reactor is not immediately shutdown [1]. It is very important to monitor and predict the DNB Ratio (DNBR) to prevent the boiling crisis and clad melting. Here, the DNB Ratio (DNBR) is defined as the ratio of the expected critical heat flux (CHF) to the actual fuel rod heat flux. So far, lots of researches have been carried out on the prediction of DNBR values [2-7].

In this thesis, a correlation limit DNBR is established based on the variance of the correlation such that there is a 95% probability at 95% confidence levels that DNB will not take place when the calculated DNBR is at the correlation limit DNBR. The variable value design method presumes that the DNBR on the limiting power rod is greater than the correlation limit DNBR by statistically combining the effects of uncertainties of the input parameters. The design limit DNBR is determined by utilizing the DNBR sensitivities and variances in three input parameter categories: plant operating parameters, nuclear and thermal parameters, and fabrication parameters [8].

OPR1000 and APR1400 which are nuclear reactors developed by Korea hydro and nuclear power company (KHNP), employ the Core Operating Limit Supervisory System (COLSS) for monitoring and the Core Protection Calculator System (CPCS) for protection. These systems continuously calculate DNBR and Local Power Density (LPD) in order to assure that the specified acceptable fuel design limits on DNB and centerline melt are not exceeded during anticipated operational

occurrences. The CPCS calculates faster than COLSS but produces more conservative values than COLSS. Even though the COLSS calculates more accurate DNBR than the CPCS, the COLSS calculates the minimum DNBR (MDNBR) using the pseudo hot rod axial power distribution which is defined as multiplication of the core average axial power distribution and the planewise peaking factor according to the control rod configuration. Therefore, the pseudo hot rod axial power distribution is different from the real hot rod axial power distribution in the reactor core and the MDNBR is usually underestimated about 35% as much as best-estimated DNBR. If the proposed algorithm can predict the DNBR within about 10% error, it will be successful.

A number of mathematical algorithms requiring high precision have been studied to solve engineering system problems, such as monitoring and diagnostics. Artificial intelligence methods have been extensively and successfully applied to nonlinear function approximation such as the problem in question for predicting DNBR values, which are a function of various input variables [3], [6], [9], [10], [11]. Among them, this work employed the support vector regression (SVR) model to predict axial DNBR distribution in the reactor core based on measured signals from the reactor coolant system. Also, the proposed DNB estimation algorithm is verified by using nuclear and thermal data [10] acquired from lots of numerical simulations of the Yonggwang nuclear power plant unit 3 (YGN-3). The used input data are the reactor power, the core inlet temperature, the pressurizer pressure, the coolant flowrate of the reactor core, the axial shape index (ASI), a variety of control rod positions and the output data is DNBR values at each axial location of a hot rod. Also, hot rod DNB data was obtained by running the MASTER [12] and COBRA [13] codes.

Ⅱ. Support Vector Regression

A. Model Development

Currently, on-line monitoring techniques using artificial intelligence are explained in literatures [14-15] on applications to a nuclear engineering field. The SVMs are an alternative training method using a kernel function for an artificial neural network (ANN) and are useful for recognizing subtle patterns in complex data sets. Generally, The SVMs are trained with a learning algorithm that originates from theoretical foundations of statistical learning theory and structural risk minimization (SRM). Figure 1 depicts the SRM principle graphically [16]. The risk bound is the sum of the empirical risk and the confidence interval. Empirical risk minimization (ERM) methods only depend on minimizing the empirical risk under no circumstances, whereas SRM methods finds the function f^* that gives the smallest guaranteed risk $R(f^*)$ for the given data set. In Figure 1, d_k denotes the dimension of the set of functions of the learning machines. A structure on the set of functions is determined by the nested subsets of functions; $S_1 \subset S_2 \subset S_3 \subset \cdots$. Any element S_i of structrue has a finite dimension d_i. The difference in risk minimization leads to better generalization in SVMs than ANNs [16].

ANNs use conventional ERM principle to minimize approximation errors of the training data. On the other hand, SVMs use an SRM principle to minimize the upper bound of the expected risk, which enables SVMs to have an optimum structure. But in case that there are many training data, SVMs require long training time. But after completion of training, there is no difference in the calculation time of DNBR which is too fast. The SVMs can be well applied to regression and classification problems. In other words, there are two main categories for support vector machines: support vector classification (SVC) and support vector regression (SVR). This thesis solves a typical regression problem

which is to approximate an unknown function, which can be expressed as a linear expansion of basis functions.

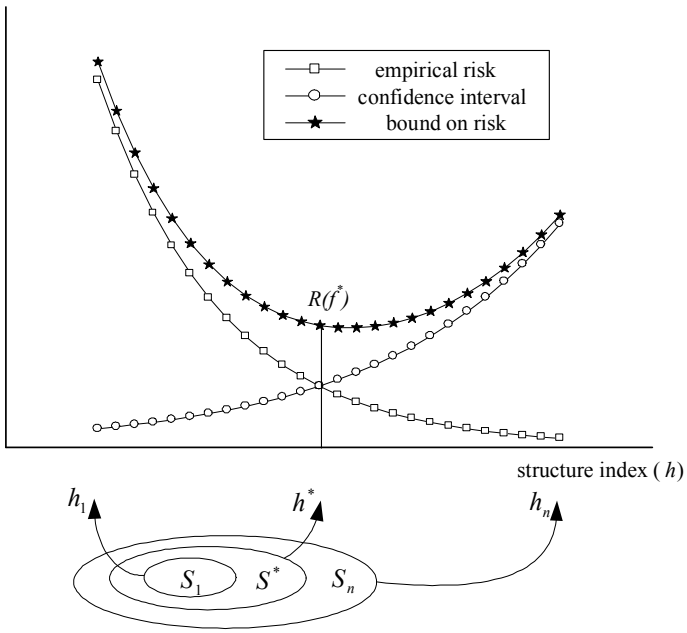

Fig. 1. Graphical description of the SRM principle

An SVR model learns a relationship between the inputs and the output from the training data set $\{(\boldsymbol{x_i}, y_i)\}_{i=1}^{N} \in R^m \times R$ where $\boldsymbol{x_i}$ is the input vector to an SVR model, y_i the actual output value, N the total number of data, and m the number of input signals. The support vector approximation is expanded as follows:

$$y = f(\boldsymbol{x}) = \sum_{i=1}^{N} w_i \phi_i(\boldsymbol{x}) + b = \boldsymbol{w}^T \boldsymbol{\phi}(\boldsymbol{x}) + b \tag{1}$$

where

$\boldsymbol{w} = [w_1 \; w_2 \; \cdots \; w_N]^T$,

$\boldsymbol{\phi} = [\phi_1 \; \phi_2 \; \cdots \; \phi_N]^T$.

After input vectors $\boldsymbol{x}$ are mapped into vectors $\boldsymbol{\phi}$ of the multidimensional kernel-induced feature space, the nonlinear regression model turns into a linear regression model in the feature space. The function $\phi_i(\boldsymbol{x})$ is called the feature, and parameters $\boldsymbol{w}$ and b are support vector weight and bias, which are calculated by minimizing the following regularized risk function [16]:

$$R(\boldsymbol{w}) = \frac{1}{2}\boldsymbol{w}^T\boldsymbol{w} + \lambda\sum_{i=1}^{N}\left|y_i - f(\boldsymbol{x})\right|_\epsilon \tag{2}$$

where

$$|y_i - f(\boldsymbol{x})|_\epsilon = \begin{cases} 0 & \text{if} \quad \left|y_i - f(\boldsymbol{x})\right| < \epsilon \\ \left|y_i - f(\boldsymbol{x})\right| - \epsilon & otherwise \end{cases} \tag{3}$$

In Eq. (2), the first term is a weight vector norm that is characterized as model complexity and the second term is an approximation error. The constant λ which is one of the user-specified parameters is known as the regularization parameter. The regularization parameter determines the trade-off between the approximation error and the weight vector norm. Also, the function $\left|y_i - f(\boldsymbol{x})\right|_\epsilon$ using another user-specified parameter ϵ is called the ϵ-insensitive loss function [17]. The loss equals zero if the predicted value $f(\boldsymbol{x})$ falls inside the insensitivity zone ϵ, that means that the predicted value is within the insensitivity zone. For all other estimated points outside the error level, ϵ, the loss is equal to the magnitude of the difference between the estimated value and ϵ (see Fig. 2 and 3)

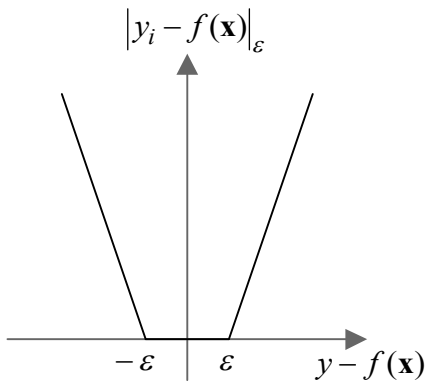

Fig. 2. Linear ϵ-insensitive loss function

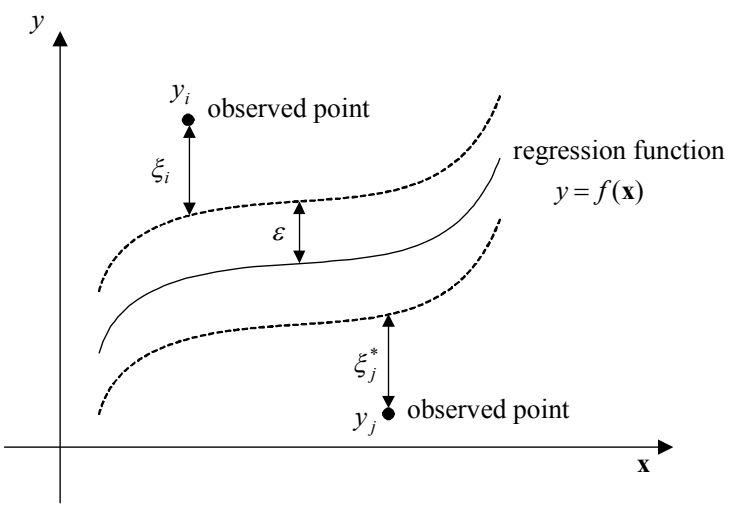

Fig. 3. Insensitive ϵ-tube for the SVR model

Minimizing the regularized risk function is equivalent to minimizing the following constrained risk function:

$$R(\boldsymbol{w},\xi,\xi^*)=\frac{1}{2}\boldsymbol{w}^T\boldsymbol{w}+\lambda\sum_{i=1}^{N}(\xi_i+\xi_i^*) \tag{4}$$

subject to the constraint

$$\begin{cases} y_i-\boldsymbol{w}^T\boldsymbol{\phi}(\boldsymbol{x})-b\le\epsilon+\xi_i, & i=1,2,\cdots,N \\ \boldsymbol{w}^T\boldsymbol{\phi}(\boldsymbol{x})+b-y_i\le\epsilon+\xi_i^*, & i=1,2,\cdots,N \\ \xi_i,\ \xi_i^*\ge 0, & i=1,2,\cdots,N \end{cases} \tag{5}$$

where

$$\boldsymbol{\xi}=[\xi_1\ \ \xi_2\ \ \cdots\ \ \xi_N]^T,$$

$$\boldsymbol{\xi}^*=[\xi_1^*\ \ \xi_2^*\ \ \cdots\ \ \xi_N^*]^T$$

The parameters ξ_i and ξ_i^* are the slack variables that represent the upper and lower constraints on the output of the system, respectively, and are positive values (refer to Fig. 3).

The constrained optimization problem can be solved by applying the Lagrange multiplier technique to Eqs. (4) and (5), which is expressed by the following Lagrange functional:

$$\begin{aligned}\Phi(\boldsymbol{w},b,\xi_i,\xi_i^*,\alpha_i\alpha_i^*,\beta_i,\beta_i^*)=&\frac{1}{2}\boldsymbol{w}^T\boldsymbol{w}+\lambda\sum_{i=1}^{N}(\xi_i+\xi_i^*)-\sum_{i=1}^{N}\alpha_i[\boldsymbol{w}^T\boldsymbol{\phi}(\boldsymbol{x}_i)+b-y_i+\epsilon+\xi_i] \\ &-\sum_{i=1}^{N}\alpha_i^*[y_i-\boldsymbol{w}^T\boldsymbol{\phi}(\boldsymbol{x}_i)-b+\epsilon+\xi_i^*]-\sum_{i=1}^{N}(\beta_i\xi_i+\beta_i^*\xi_i^*)\end{aligned} \tag{6}$$

Minimizing Eq. (6) with respect to the primal variables, $\boldsymbol{w},b,\xi_i,\xi_i^*$, gives the following conditions:

$$\boldsymbol{w}=\sum_{i=1}^{N}(\alpha_i-\alpha_i^*)\boldsymbol{\phi}(\boldsymbol{x}_i) \tag{7}$$

$$\sum_{i=1}^{N}(\alpha_i-\alpha_i^*)=0$$

$$\lambda-\alpha_i-\beta_i=0,\ i=1,2,\ \cdots,N$$

$$\lambda-\alpha_i^*-\beta_i^*=0,\ i=1,2,\ \cdots,N$$

Lagrange function is calculated by Eq. (7) as following:

$$\Psi(\alpha_i,\alpha_i^*)=\sum_{i=1}^{N}y_i(\alpha_i-\alpha_i^*)-\epsilon\sum_{i=1}^{N}(\alpha_i+\alpha_i^*)-\frac{1}{2}\sum_{i=1}^{N}\sum_{j=1}^{N}(\alpha_i-\alpha_i^*)(\alpha_j-\alpha_j^*)\boldsymbol{\phi}^T(\boldsymbol{x}_i)\boldsymbol{\phi}(\boldsymbol{x}_j) \tag{8}$$

subject to the constraints

$$\begin{cases}\displaystyle\sum_{i=1}^{N}(\alpha_i-\alpha_i^*)=0\\ 0\le\alpha_i\le\lambda,\ i=1,2,\ \cdots,N\\ 0\le\alpha_i^*\le\lambda,\ i=1,2,\ \cdots,N\end{cases} \tag{9}$$

The above Lagrange functional can be solved by determining the values for α_i and α_i^* using a quadratic programming technique. Finally, the regression function of Eq. (1) is expressed as follows:

$$y=f(\boldsymbol{x})=\sum_{i=1}^{N}(\alpha_i-\alpha_i^*)K(\boldsymbol{x},\boldsymbol{x}_i)+b=\sum_{i=1}^{N}\gamma_iK(\boldsymbol{x},\boldsymbol{x}_i)+b \tag{10}$$

where $K(\boldsymbol{x},\boldsymbol{x}_i)=\boldsymbol{\phi}^{\boldsymbol{T}}(\boldsymbol{x_i})\boldsymbol{\phi}(\boldsymbol{x})$ is known as kernel function. A lot of coefficients $\gamma_i=(\alpha_i-\alpha_i^*)$ have nonzero values and the corresponding training data points are known as support vectors (SVs) that have an approximation error that is greater than or equal to ϵ. In this thesis, we use the following radial basis function:

$$K(\boldsymbol{x},\boldsymbol{x}_i)=\exp\left(-\frac{(\boldsymbol{x}-\boldsymbol{x}_i^T)(\boldsymbol{x}-\boldsymbol{x}_i)}{2\sigma^2}\right) \tag{11}$$

The kernel function parameter determines the sharpness of the radial basis kernel function. The bias b is calculated as [17]

$$b = -\frac{1}{2}\sum_{i=1}^{N}\gamma_i\left(K(\boldsymbol{x_r}, \boldsymbol{x_i}) + K(\boldsymbol{x_s}, \boldsymbol{x_i})\right) \tag{12}$$

where $\boldsymbol{x}_r$ and $\boldsymbol{x}_s$ are SVs and these are data points outside the ϵ-insensitivityzone.

The Two most relevant design parameters for the SVR model are regularization parameter λ and the insensitivity zone ϵ. An increase of the parameter λ reduces larger errors, which leads to a decrease in an approximation error. This can be achieved by increasing the weights vector norm. However, an increase in the weight vector norm does not make sure of the good generalization performance of the SVR model. An increase in the insensitivity zone ϵ means a reduction in requirements for the approximation accuracy and it also decreases the number of support vectors, leading to data compression.

B. Selection of the Training Data

An SVR model can be well trained when we use data that include much information. In this thesis, a subtractive clustering (SC) scheme is adopted to select the training data set. The SC scheme introduces the concept of the information potential. The information potential of each data point indicates the information quantity and it is expected that a data point with high information potential has much information. Figure 4 shows data clusters and their centers (indicated as '+' signs) for simple two-dimensional data.

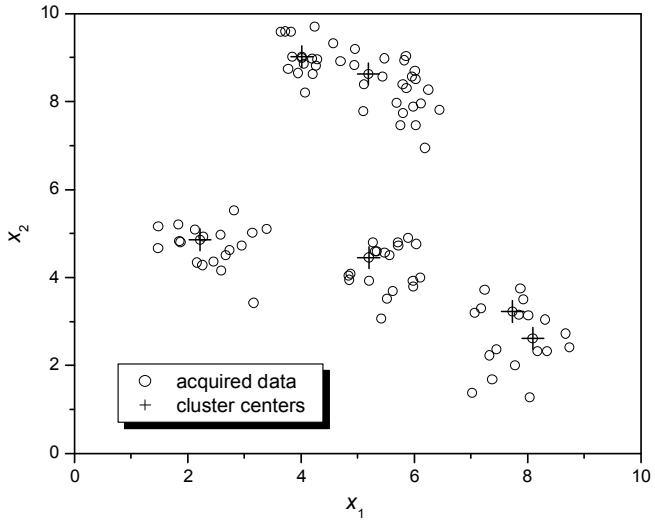

Fig. 4. Data clusters and cluster centers for simple two-dimensional data

The information potential of each data point is defined as a function of the Euclidean distances to all other input data points [18].

$$P_1(i) = \sum_{j=1}^{N} e^{-4\|\boldsymbol{x}_i - \boldsymbol{x}_j\|^2 / r_\alpha^2},\ i = 1,2,\cdots,N \tag{13}$$

where a positive constant r_α is a radius defining a particular neighborhood of the cluster. The potential of a data point to be cluster center is higher when it is surrounded by an amount of neighboring data. After calculating the potential of each data point, the data point with the highest potential is considered as first cluster center. Each time a cluster center is obtained. In general, after determining the k-th cluster center $\boldsymbol{c}_k$ and its potential value P_k^c, the potential of each data point is recalculated using the following equation:

$$P_{k+1}(i) = P_k(i) - P_k^c e^{-4\|\boldsymbol{x}_i - \boldsymbol{x}_k^c\|^2 / r_\beta^2},\ i = 1,2,\cdots,N \tag{14}$$

where a positive constant r_β denotes radius of the neighborhood. Also, r_β is

usually greater than r_α in order to limit the number of clusters generated. When the potentials of all data points are recalculated using Eq. (14), the data point with the highest potential is selected as the $(k+1)^{\text{th}}$ cluster center. The calculation stops if $P_k^c < \zeta P_1^c$ is true, otherwise calculation continues. If the calculation stops at an iterative step N_c, this means there are N_c cluster centers. The input/output data positioned in cluster centers are selected to train the SVR model.

Ⅲ. Verification of the Proposed Algorithm

The proposed SVR model was applied to the first fuel cycle of the YGN-3, a prototype plant of OPR 1000 nuclear plants. The axial DNB distribution data of the hot fuel rod were obtained by running MASTER (Multipurpose Analyzer for Static and Transient Effects of Reactor) [12] and COBRA [13] codes. The MASTER code which was developed by Korea Atomic Energy Research Institute (KAERI) is a nuclear analysis and design code. The MASTER code has a variety of capabilities such as static core design, transient core analysis and operation support and is interfaced with COBRA code for thermo-hydraulic calculations. The COBRA code has the CE-1 critical heat flux (CHF) correlation and the DNB distribution data are calculated from this CHF correlation.

The hot rod DNB data from MASTER simulations consist of a total of 18816 input-output data pairs $(x_1, x_2, \cdots x_9, y_r)$. x_1 through x_9 are input signals, which represent the reactor power, core inlet temperature, coolant pressure, coolant mass flowrate, ASI, R2, R3, R4 and R5 control rod positions. Here, R2, R3, R4 and R5 stand for the names of the control rod banks. y_r is DNBR values at each axial location of a hot nuclear fuel rod and calculated from ex-core neutron sensors. The hot fuel rod is determined from 3-dimensional core calculation. Figure 5 shows DNBR trends according to the input variables such as reactor power, coolant inlet temperature, coolant pressure, and coolant mass flowrate that affect the DNBR value.

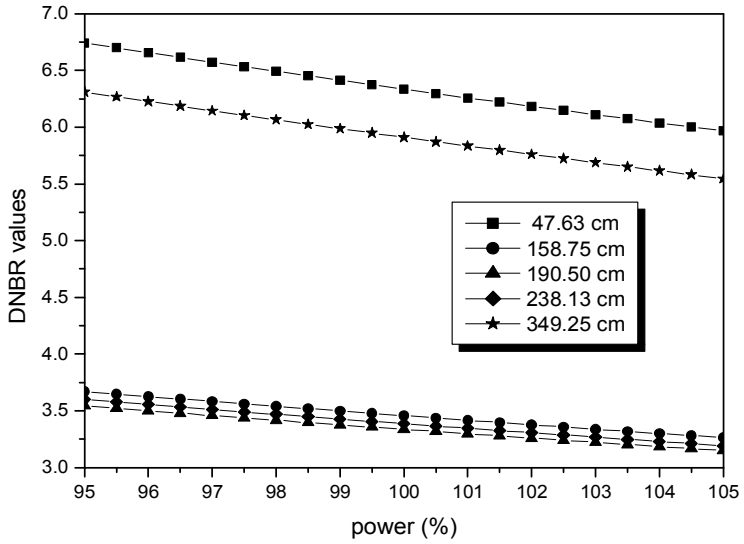

(a) power

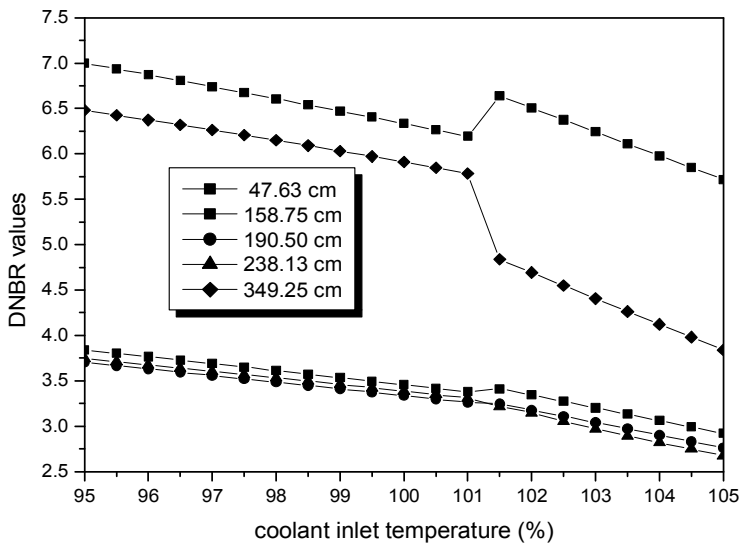

(b) inlet coolant temperature

Fig. 5. Effect of input variables on DNBR

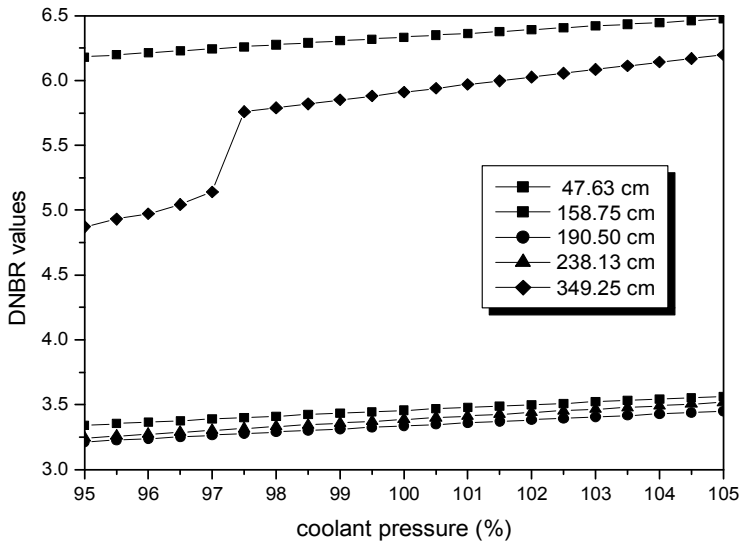

(c) coolant pressure

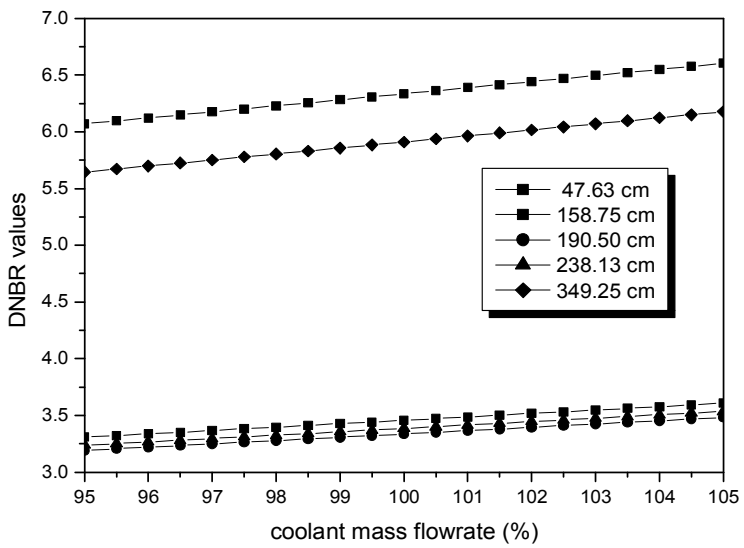

(d) reactor coolant mass flowrate

Fig. 5. Contiuned

The ASI and the control rod position affect the axial power distribution of the hot fuel rod that has a close relationship with DNBR distribution. The ASI is defined as $\frac{P_B - P_T}{P_B + P_T}$ where P_B is a bottom part power of a reactor core and P_T is a top part power. When the input values change in each specific range, DNBR values of the hot fuel rod are obtained. The ranges of the input signals that are used for training are shown in Table 1.

Table 1. Input signal ranges

Input signals	Nominal values	Ranges
Reactor power (%)	100%	80 ~ 103
Inlet temperature (℃)	295.8	290.6 ~ 301.7
Pressure (bar)	155.17	131.0 ~ 160.0
Mass flowrate (kg/m^2-sec)	3565.0	2994.6 ~ 4135.4
R2 control rod positions (cm)	-	0 ~ 381
R3 control rod positions (cm)	-	0 ~ 381
R4 control rod positions (cm)	-	0 ~ 381
R5 control rod positions (cm)	-	0 ~ 381
Axial shape index	-	-0.534 ~ 0.432

The DNB data are divided into the training and test data sets using the SC scheme. The training data set comprise a half of the acquired input and output data pairs and the test data set comprises a half of the total DNB data, which means that the number of the test data are the same as that of the training data. The training data are sampled to incorporate the whole input ranges shown in

Table 1. The correlation between ASI and DNBR is largest among any other input variable. Therefore, two different types of SVR models are used for DNBR data that are divided into two ASI cases; one positive ASI (9408 data points) case and another negative ASI case (9408 data points) which takes on different aspects, respectively. A total of 26 SVR models are designed to estimate the DNBR for both positive and negative ASIs at 13 axial locations ($26 = 13 \times 2$). The parameters of the SVR models used in this thesis are $\epsilon = 0.01$, $\lambda = 10$ and $\sigma = 5$. These parameters can be easily chosen through numerical simulations.

The DNBR value of 13 axial positions is calculated by the SVR models starting from the bottom of a hot rod to the top. It is expected that if we use the DNBR value pre-estimated for the one step lower axial location of a hot rod as an input of the SVR models, the errors can be decreased. Therefore, this pre-estimated DNBR value would be used. Table 2 shows the RMS errors calculated by SVR models at 13 axial positions. It is be shown from this table that the proposed algorithm estimates DNBR values for negative ASI better than positive ASI and that the errors of the estimated DNBR values become relatively high at the top locations of the hot rod for the positive ASI values.

Table 2. RMS error calculated by SVR models at 13 axial positions

	Non pre-estimated				Pre-estimated			
	Training data		Test data		Training data		Test data	
Axial position	Positive ASI	Negative ASI	Positive ASI	Negative ASI	Positive ASI	Negative ASI	Positive ASI	Negative ASI
47.63	1.2371	1.1364	1.4894	1.2665	1.2371	1.1363	1.4894	1.2665
95.25	0.8997	1.0017	1.0668	1.0988	0.8919	0.7559	1.0055	0.9969
142.88	0.5866	0.7372	0.6453	0.7900	0.5870	0.6929	0.6171	0.7265
158.75	0.5189	0.5822	0.5197	0.6852	0.3831	0.5022	0.4998	0.6721
174.63	0.4811	0.5545	0.4272	0.6016	0.3480	0.5122	0.4388	0.5992
190.5	0.4831	0.4792	0.4089	0.5388	0.4061	0.4573	0.4616	0.5414
206.38	0.6741	0.4817	0.6310	0.5056	0.5286	0.4332	0.5869	0.5262
222.25	0.8420	0.4506	0.8560	0.4760	0.7164	0.3561	0.7646	0.4771
238.13	1.1263	0.4048	1.1745	0.4534	1.0724	0.3778	1.0004	0.4675
254.00	1.4011	0.3691	1.4903	0.3986	1.3332	0.3487	1.2040	0.4430
269.88	1.6487	0.3470	1.7785	0.3810	1.5590	0.3264	1.4506	0.4195
301.63	2.2471	0.3610	2.5345	0.4215	2.0416	0.3471	2.1016	0.4263
349.25	3.3670	1.0689	3.9665	1.2023	3.2032	0.9782	3.3682	1.0918

Figure 6 shows the relative DNBR error distribution at an axial mid-position (190.5cm) of a hot rod of which length is 381cm. The relative error is defined as $\frac{|y_r - \hat{y}|}{y_r}$ where $\hat{y}$ is an estimated value and y_r is a target value.

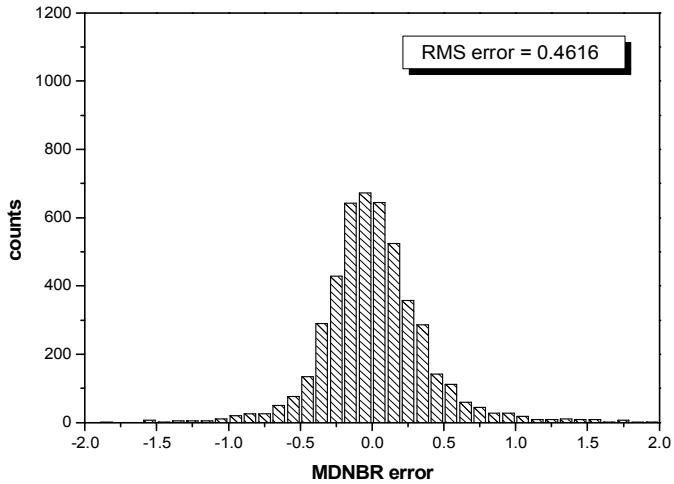

(a) postive ASI

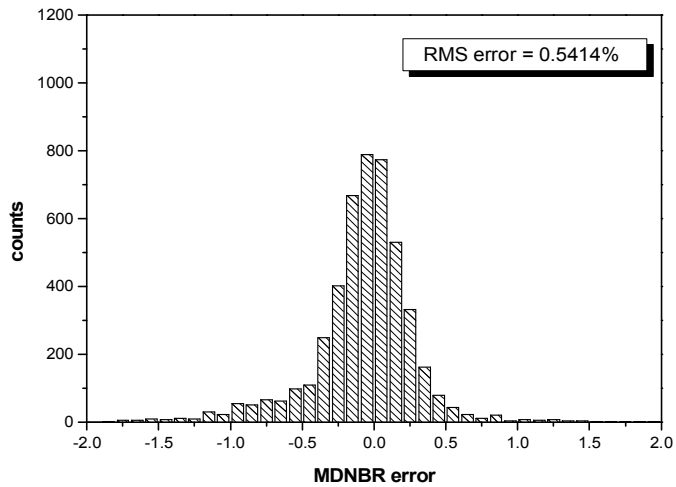

(b) negative ASI

Fig. 6. Relative DNBR error distribution at an axial mid-position (190.5) of a hot rod

Figure 7 shows the root mean square (RMS) errors of DNBR values and compares both results that use or do not use the pre-estimated DNBR values. When the pre-estimated signals are used, the RMS error is smaller than when the pre-estimated signals are not used.

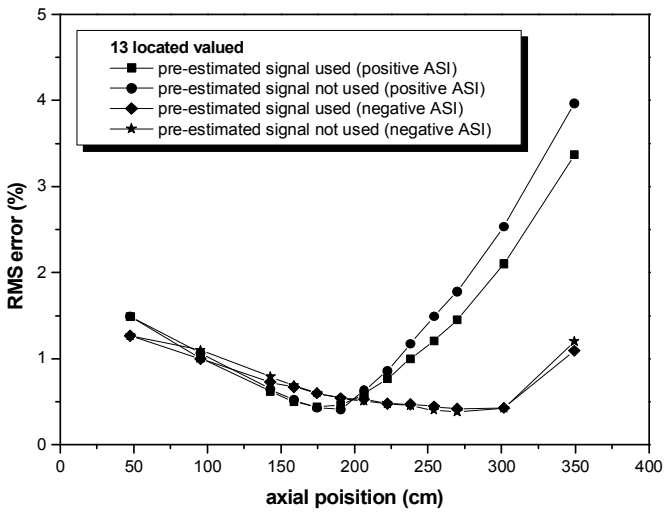

Fig. 7. Effect of using pre-estimated signals

Figure 8 shows the RMS error and the maximum error at each axial location. For the training data set, the RMS errors averaged for 13 axial locations of the hot rod are 1.1006 percent for positive ASI values and 0.5572 percent for negative ASI values. For the test data set, the RMS errors averaged at 13 different axial locations of the hot rod are 1.1530 percent for positive ASI values and 0.6657 percent for negative ASI values. The maximum errors are not as important as the RMS errors and are graphed to show that the maximum value could be high at a specific operating condition but is not so high.

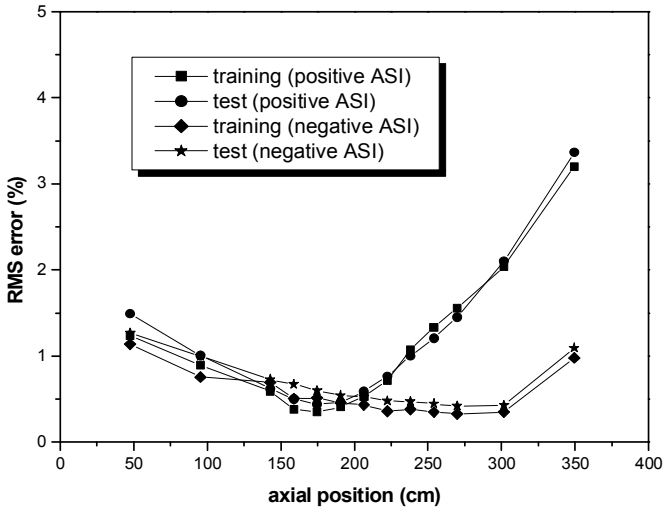

(a) RMS errors

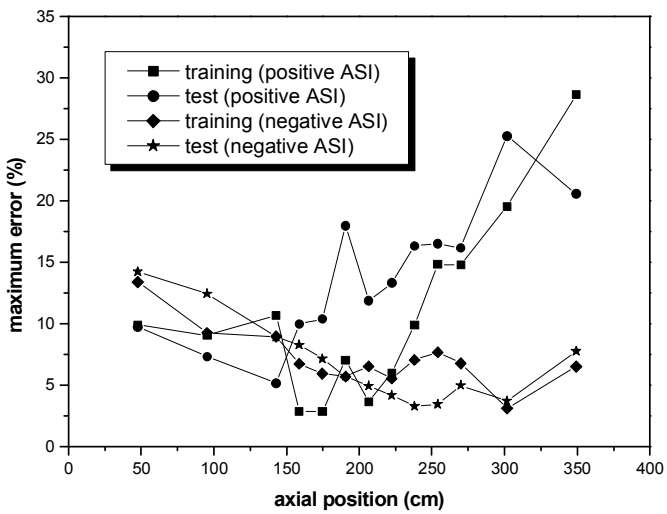

(b) maximum error

Fig. 8. Errors for training and test data at respective axial locations

The numerical values shown in Table 3 indicate two kinds (RMS and maximum) of the errors that average the DNBR errors for 13 axial positions of the hot rod where indicates the maximum or RMS errors at each axial location. As shown in this table, if both the ASI and the pre-estimated DNBR values are used as inputs of the SVR models, the performance is best comparing to cases they are not used. Also, it is known that the RMS error of the SVR for the test data is almost the same as RMS error for the training data. Therefore, if the SVR models are trained first using the data for various operating conditions, it can accurately predict the DNBR for any other operating data.

Table 3. DNBR estimation results

Application range	Pre-estimated	Errors (Training data)		Errors (Test data)	
		RMS error (%)	Max. error (%)	RMS error (%)	Max. error (%)
Positive ASI	No	1.1933	12.2599	1.3068	13.6065
	Yes	1.1006	10.7495	1.1530	13.8966
Negative ASI	No	0.6134	8.5802	0.6784	6.5997
	Yes	0.5572	7.1672	0.6657	6.8540
Total	No	0.9034	10.4201	0.9926	10.1031
	Yes	0.8289	8.9584	0.9094	10.3753

As an example of the prediction performance, figure 9 shows the target DNBR and the estimated DNBR distribution at the hot rod position for one specific case (for an operating condition in the test data). It is shown that the proposed SVR models can estimate well the reference DNBR.

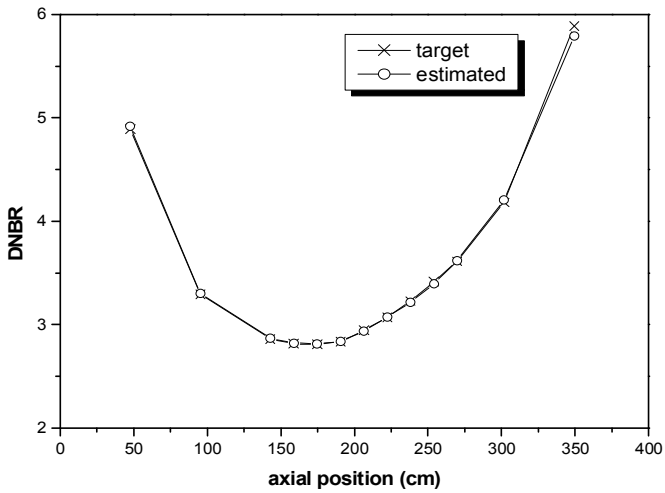

(a) positive ASI

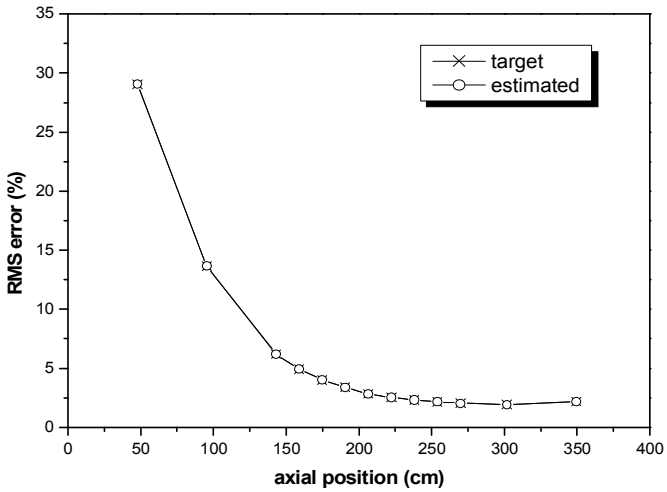

(b) negative ASI

Fig. 9. Estimation of axial DNBR distribution at the hot rod position for a specific operating condition

In addition, DNBR distribution trends due to a transient event are shown Figure 10. The transient was induced by the R5 control bank ejection from steady state 85 percent power (the R5 bank position was 280 cm and all other control banks were ejected). Although the RMS error level is relatively high at higher DNBR values, it is known that the proposed method estimate well the DNBR distribution for the transient event. It is important to estimate well the DNBR values at the lowest DNBR positions in safety aspects and it can be inferred from Figure 8 that the proposed algorithm predict DNBR at the lower DNBR positions more accurately.

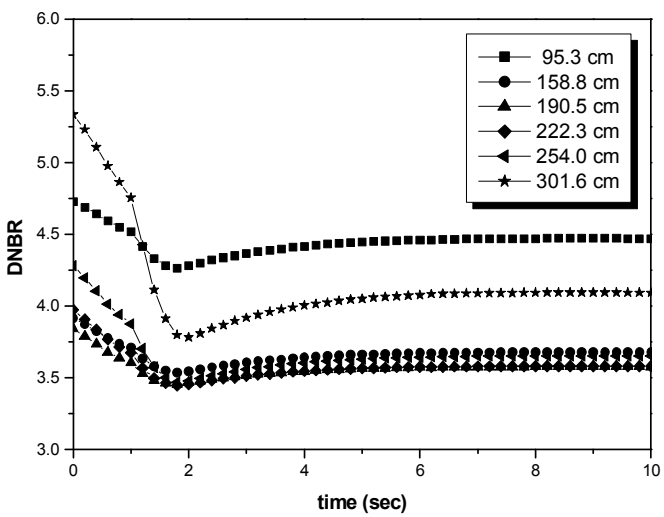

(a) estimated DNBR

Fig. 10. DNBR distribution trends for a transient case

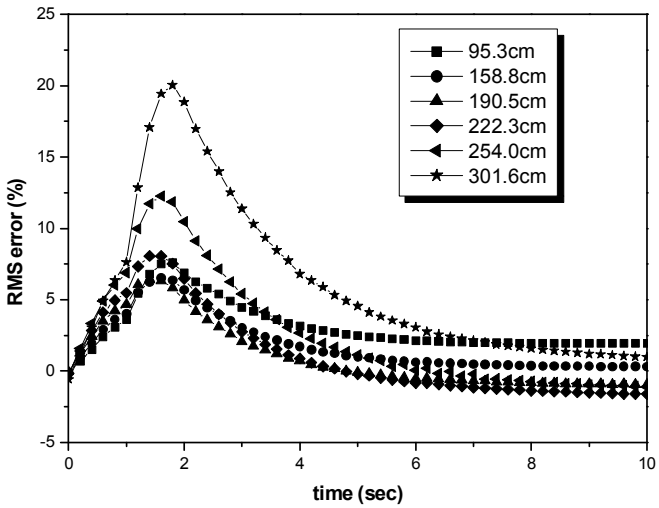

(b) estimated DNBR error

Fig. 10. Continued

Table 4 shows the comparison of the proposed SVR method with previously studied fuzzy neural network (FNN) [19]. Note that SVR and FNN [19] used the same data and conditions. Comparing the prediction performance for developed two models, it is from the Table 4 known that the SVR method is slightly superior to the FNN method.

Table 4. Comparison of the performance for two developed models (FNN, SVR)

Model	Pre-estimated	Errors (Training data)		Errors (Test data)	
		RMS Error (%)	Max. Error (%)	RMS Error (%)	Max. Error (%)
FNN	No	1.1315	15.4977	1.0894	18.0101
	Yes	1.0603	15.3731	1.0397	19.8579
SVR	No	0.9034	10.4201	0.9926	10.1031
	Yes	0.8289	8.9584	0.9094	10.3753

Ⅳ. Conclusions

In this thesis, SVR models have been developed to estimate the DNBR distribution at respective axial locations of the hot nuclear fuel rod in a reactor core. Two different types of SVR models are used for DNBR data that are divided into positive and negative ASIs, which takes on different aspects. The SVR models have been trained by using training data set and verified by using the test data set independent from the training data. The developed SVR models have been applied to the first fuel cycle of the Yonggwang unit 3 PWR plant. The simulation results show that using the pre-estimated DNBR data slightly reduce the prediction errors compared to when the pre-estimated DNBR data are not used. The errors of the training and test data sets are almost the same, which means that once SVR models are trained, the SVR models can be applied to estimate the DNBR in a reactor core for any other operating data. In addition, the proposed method estimated well the DNBR distribution for the transient event. From this application, it was known that this algorithm can predict the DNBR distribution accurately each time step and provide reliable protection and monitoring information for the nuclear power plant operation.

References

[1] L. S. Tong, “An evaluation of the departure from nucleate boiling in bundles of reactor fuel rods,” Nucl. Sci. Eng, Vol. 33, pp. 7-15 (1968).

[2] H. K. Kim, S. H. Lee, and S. H. Chang, “Neural network model for estimating departure from nucleate boiling performance of a pressurized water reactor core,” Nucl. Tech., Vol. 101, No. 2, pp. 111-121 (1993).

[3] H. C. Kim and S. H. Chang, “Development of a back propagation network for one-step transient DNBR calculations,” Ann. Nucl. Energy, Vol. 24, No. 17, pp. 1437-1446 (1997).

[4] J. K. Lee and B. S. Han, “Modeling of core protection and monitoring system for PWR nuclear power plant simulator,” Ann. Nucl. Energy, Vol. 25, No. 7, pp. 409-420 (1998).

[5] M. G. Na, “Application of a genetic neuro-fuzzy logic to departure from nucleate boiling protection limit estimation,” Nucl. Tech., Vol. 128, No. 3, pp. 327-340, (1999).

[6] M. G. Na, “DNB limit estimation using an adaptive fuzzy inference system,” IEEE Trans. Nucl. Sci., Vol. 47, No. 6, pp. 1948-1953 (2000).

[7] W. K. In, D. H. Hwang, Y. J. Yoo, and S. Q. Zee, “Assessment of core protection and monitoring systems for an advanced reactor SMART,” Ann. Nucl Energy, Vol. 29, pp. 609-621 (2002).

[8] H. Chelemer, L.H. Boman, and D.R. Sharp, Improved Thermal Design Procedure. WCAP-8567 (1975).

[9] M. G. Na, “On-line estimation of DNB protection limit via a fuzzy neural network,” Nucl. Eng. Tech., Vol. 30, No. 3, pp. 222 - 234 (1998).

[10] M. G. Na, S. M. Lee, S. H. Shin, D. W. Jung, K. B. Lee, and Y.J. Lee, “Minimum DNBR monitoring using fuzzy neural networks,” Nucl. Eng. Des., Vol. 234, No. 1-3, pp. 147 - 155 (2004).

[11] G. C. Lee and S. H. Chang, “Radial basis function networks applied to DNBR calculation in digital core protection systems,” Ann. Nucl. Energy, Vol. 30, No. 15, pp. 1561 – 1572 (2003).

[12] B. O. Cho, et al., MASTER-2.0: Multi-purpose Analyzer for Static and Transient Effects of Reactors. KAERI, KAERI/TR-1211/99 (1999).

[13] C. L. Wheeler, et al., COBRA-IV-I; An Interim Version of COBRA for Thermal Hydraulic Analysis of Rod Bundle Nuclear Fuel Elements and Cores. BNWL-1962 (1976).

[14] J. Garvey, D. Garvey, R. Seibert, and J.W. Hines, “Validation of on-line monitoring techniques to nuclear plant data,” Nucl. Eng. Tech., Vol. 39, No. 2, pp. 149-158 (2007).

[15] G.Y. Heo, “Condition monitoring using empirical models: technical review and prospects for nuclear applications,” Nucl. Eng. Tech., Vol. 40, No. 1, pp. 49-68 (2008).

[16] V. N. Vapnik, Statistical Learning Theory, Wiley, New York (1998).

[17] V. N. Vapnik, The Nature of Statistical Learning Theory, Springer, New York (1995).

[18] S. L. Chiu, “Fuzzy model identification based on cluster estimation,” J. Intell. Fuzzy Syst., Vol. 2, No. 3, pp. 267 – 278 (1994).

[19] M. G. Na, S. M. Lee, S. H. Shin, D. W. Jung, K. B. Lee, and Y.J. Lee, “Estimation of Axial DNBR Distribution at the Hot Pin Position of a Reactor Core Using Fuzzy Neural Networks,” J. Nucl. Sci. Tech., Vol. 41, No. 8, pp. 817 – 826 (2004).

감사의 글

이제는 집보다 더 편해진 NICL, my Lab..!! 항상 9시 출근 10시 퇴근..! 3년간의 삶의 터전..!

처음 쳐다보지도 못할 大 고참 형들 앞에서 초라했던 내가 이제는 실험실 최고의 위치에서 대학원 생활의 끝을 상징하는 졸업논문을 쓰다니..이렇다 할 목표도 선정하지 못한 채 선택한 대학원의 생활은 아쉬움을 뒤로한 채 끝을 향해가는 지금..이러한 감사의 글을 마지막으로 나의 느낌을 표현할 수 있다는 점을 위로삼아 마지막 추억을 되짚어 보고자 합니다.

인자하면서도 때로는 엄한 아버지 같은 나의 영원한 스승님. 나만균 교수님. 교수님의 지도를 교훈삼아 행동하면 앞으로 어떠한 상황이 닥치더라도 무리 없이 해결할 수 있을 것이라는 확신이 섭니다. 특히 교수님이 계셨기에 가능했던 수많은 경험들, 사소한 것 하나까지도 신경써주신 배려는 정말 잊지 못할 것입니다. 이점 고개 숙여 감사드립니다. 학부생부터 지금까지 잊지 못할 명 강의를 해주시고, 바쁘신 와중에도 많은 관심을 가져주신 김숭평 교수님, 송종순 교수님, 정운관 교수님, 이경진 교수님, 김진원 교수님, 신원기 교수님, 이기복 교수님, 이심교 교수님 진심으로 감사드립니다.

NICL에 처음 발을 들여놓게 해준 나의 몸체 성한이형, 나를 당구세계로 이끈 인호형, 상담을 담당해준 동혁이형, 음주문화 전파자 헌영이형 모두 졸업하셨지만 아직까지도 생생합니다. 명절이나 스승의 날에만 볼 수 있는 우리 Lab의 선구자 영록이형, 선호형, 동원이형, 인준이형, 짧은 만남이지만 많은 조언을 얻었습니다. 영규, 심원, 재환, 순호, 주현 형제와도 같았던 my Lab family. 정말 고맙다. 특히 재환, 순호, 주현이 이제 Lab은 니들 하기 나름이다. 지금보다 Lab을 훨씬 훌륭하게 이끌어 나갈 수 있을 것이라 믿는다.

각자 실험실에서 대학원 생활을 같이 해오며 도와주신 유선이형, 정민이형, 용진이형, 강일이형에게 고마움을 전합니다. 믿고 의지할 수 있었던 동기 민수, 상헌, 형의 부

탁은 모두 들어 준 멋진 후배 현석, 민영, 현민, 영국아 모두 고맙다. 이외에도 많은 고마운 선, 후배 동기들이 있지만 이름을 언급하지 않았다고 해서 고마움이 덜한 것은 아닙니다. 내 삶의 원동력인 내 주변의 모든 분들 정말 감사합니다.

마지막으로 지금까지 변함없이 저를 믿어준 할머니, 아버님, 어머님, 하나뿐인 형 정말 사랑합니다.

저작물 이용 허락서

학 과	원자력공학과	학 번	20107314	과 정	석사
성 명	한글: 김 동 수 한문 : 金 東 秀 영문 : Kim Dong Su				
주 소	광주광역시 북구 각화동 금호타운 3-308				
연락처	E-MAIL : wooka109@naver.com				
논문제목	한글 : Support Vector Regression을 이용한 고온봉에서의 축방향 DNBR 분포 예측				
	영문 : Prediction of Axial DNBR Distribution in a Hot Nuclear Fuel Rod Using Support Vector Regression				

본인이 저작한 위의 저작물에 대하여 다음과 같은 조건아래 조선대학교가 저작물을 이용할 수 있도록 허락하고 동의합니다.

- 다 음 -

1. 저작물의 DB구축 및 인터넷을 포함한 정보통신망에의 공개를 위한 저작물의 복제, 기억장치에의 저장, 전송 등을 허락함
2. 위의 목적을 위하여 필요한 범위 내에서의 편집·형식상의 변경을 허락함. 다만, 저작물의 내용변경은 금지함.
3. 배포·전송된 저작물의 영리적 목적을 위한 복제, 저장, 전송 등은 금지함.
4. 저작물에 대한 이용기간은 5년으로 하고, 기간종료 3개월 이내에 별도의 의사 표시가 없을 경우에는 저작물의 이용기간을 계속 연장함.
5. 해당 저작물의 저작권을 타인에게 양도하거나 또는 출판을 허락을 하였을 경우에는 1개월 이내에 대학에 이를 통보함.
6. 조선대학교는 저작물의 이용허락 이후 해당 저작물로 인하여 발생하는 타인에 의한 권리 침해에 대하여 일체의 법적 책임을 지지 않음
7. 소속대학의 협정기관에 저작물의 제공 및 인터넷 등 정보통신망을 이용한 저작물의 전송·출력을 허락함.

동의여부 : 동의(○) 반대( )

2011년 6월 일

저작자: 김 동 수 (서명 또는 인)

조선대학교 총장 귀하